Article

Fire behaviour of modern façade materials – Understanding the Grenfell Tower fire

Mckenna, Sean Thomas, Jones, Nicola, Peck, Gabrielle, Dickens, Kathryn, Pawelec, Weronika, Oradei, Stefano, Harris, Stephen, Stec, Anna A and Hull, T Richard

Mckenna, Sean Thomas, Jones, Nicola, Peck, Gabrielle, Dickens, Kathryn, Pawelec, Weronika, Oradei, Stefano, Harris, Stephen, Stec, Anna A ORCID: 0000-0002-6861-0468 and Hull, T Richard ORCID: 0000-0002-7970-4208 (2019) Fire behaviour of modern façade materials – Understanding the Grenfell Tower fire. Journal of Hazardous Materials, 368 . pp. 115-123. ISSN 0304-3894

Journal of Hazardous Materials 368 (2019) 115–123

Contents lists available at ScienceDirect

Journal of Hazardous Materials

journal homepage: www.elsevier.com/locate/jhazmat

Fire behaviour of modern façade materials – Understanding the Grenfell Tower fire

Sean T. McKenna, Nicola Jones, Gabrielle Peck, Kathryn Dickens, Weronika Pawelec, Stefano Oradei, Stephen Harris, Anna A. Stec, T. Richard Hull*

Centre for Fire and Hazard Sciences, University of Central Lancashire, PR1 2HE, UK

ARTICLE INFO

Keywords:
Fire
Toxicity
Insulation
Building
Polymer

ABSTRACT

The 2017 Grenfell Tower fire spread rapidly around the combustible façade system on the outside of the building, killing 72 people. We used a range of micro- and bench-scale methods to understand the fire behaviour of different types of façade product, including those used on the Tower, in order to explain the speed, ferocity and lethality of the fire. Compared to the least flammable panels, polyethylene-aluminium composites showed 55x greater peak heat release rates (pHRR) and 70x greater total heat release (THR), while widely-used high-pressure laminate panels showed 25x greater pHRR and 115x greater THR. Compared to the least combustible insulation products, polyisocyanurate foam showed 16x greater pHRR and 35x greater THR, while phenolic foam showed 9x greater pHRR and 48x greater THR. A few burning drips of polyethylene from the panelling are enough to ignite the foam insulation, providing a novel explanation for rapid flame-spread within the facade. Smoke from polyisocyanurates was 15x, and phenolics 5x more toxic than from mineral wool insulation. 1 kg of burning polyisocyanurate insulation is sufficient to fill a 50m^3 room with an incapacitating and ultimately lethal effluent. Simple, additive models are proposed, which provide the same rank order as BS8414 large-scale regulatory tests.

1. Introduction

In 2006, restrictions on the use of combustible materials on the outside of tall buildings in the UK were relaxed, while targets for energy efficiency were raised. In 2016, the Grenfell Tower was refurbished with an insulated rainscreen façade system consisting of combustible polyisocyanurate (PIR) foam insulation and aluminium-polyethylene composite material, separated by a ventilated cavity (Fig. 1) covering the exterior of the building. On 14th June 2017, a fire, reported to have started in a fridge-freezer in a fourth floor apartment, broke out to ignite the recently installed façade system, after which it spread very rapidly around the outside of the building, and into almost all the other apartments, ultimately killing 72 occupants. The different components of the façade system were certified to have passed regulatory tests for fire safety, although it is arguable whether the refurbished façade system was actually compliant. The background to the fire and the regulatory regime for fire safety of tall buildings is detailed in the supplementary material (SM).

In addition to rapid fire spread around the Tower, large volumes of smoke were produced. Smoke inhalation is known to be the largest cause of death and the largest cause of injury from fire in the UK and US [1,2]. In most cases the smoke from the burning façade appears to have entered the building before the contents of each apartment ignited, so the smoke toxicity of the façade is an important factor in the tragedy. On exposure to smoke, the victim becomes incapacitated (unconscious), and unless they are rescued, death is likely to follow. Incapacitation and lethality may be estimated for 50% of an exposed population in terms of a fractional effective dose (FED), following ISO 13571 [3] (incapacitation) or ISO 13344 [4] (lethality). When the FED equals 1, the equations predict that half of the exposed population would be incapacitated or killed. Fire safety engineers may use a precautionary factor of 10 (i.e. FED $<$ 0.1) to ensure the life safety of occupants in the event of fire.

Fire toxicity is a function of both material and fire condition. It has been shown that the yield of major asphyxiants hydrogen cyanide (HCN) and carbon monoxide (CO) increases by a factor of 5 to 20 as the fire grows from well-ventilated to under-ventilated [5]. The steady state tube furnace (ISO TS 19700) [6] has been specifically designed to replicate the smoke toxicity of individual fire stages [7]. The ventilation condition of burning polyethene (PE), pouring out of the aluminium

* Corresponding author.
E-mail address: trhull@uclan.ac.uk (T.R. Hull).

https://doi.org/10.1016/j.jhazmat.2018.12.077
Received 25 September 2018; Received in revised form 14 December 2018; Accepted 20 December 2018
Available online 29 December 2018

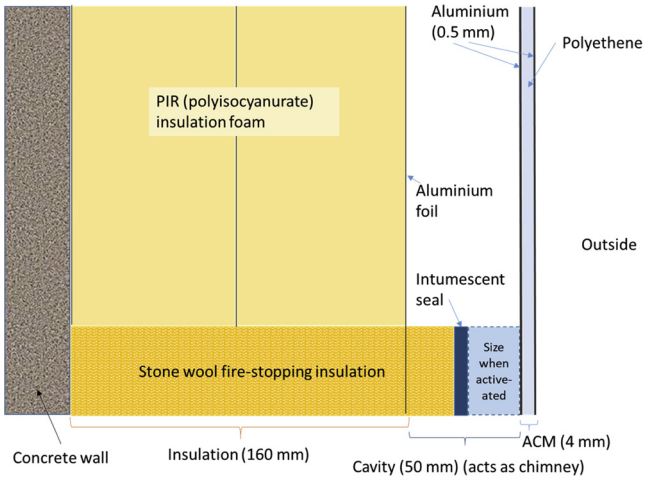

Fig. 1. Façade system in the Grenfell Tower.

composite material (ACM) screens is uncertain, while the insulation foams behind the ACM will have undergone the more toxic under-ventilated burning. Woolley and Raftery reported the increasing danger of smoke toxicity over 40 years ago [8], specifically highlighting the release of HCN from rigid and flexible urethane foams. It has been shown that when PIR foam burns it generates HCN and CO in dangerous quantities [9]. Investigation reports have shown that almost all of the Grenfell Tower occupants who died in the building collapsed because the fumes prevented escape [10]. Several survivors were treated for cyanide poisoning, and many victims had collapsed on the stairs.

The refurbishment of tall concrete buildings often involves covering the exterior with a rainscreen facade system, consisting of an outer-screen, a cavity and an inner layer of insulation. The outer-screen may be aluminium composite material (ACM), high-pressure laminate (HPL), or mineral fibre board. ACM consists of two thin sheets of aluminium (˜ 0.5 mm) sandwiching a layer of polymer (usually PE), PE filled with metal hydroxide fire retardant (FR), or predominantly non-combustible (NC), as inorganic composite or metallic filling. FR panels contain around 65% aluminium hydroxide or magnesium hydroxide, having a fire retarding effect through endothermic dehydration and the subsequent release of water, to suppress flaming [11].

At the time of the fire, two phenolic foams (PF) and one PIR foam were certified to be compliant with the UK building regulations for tall building exteriors. The certificates for the PIR foam and one phenolic foam have subsequently been withdrawn by their manufacturers. In this study, various outer-screens, and the certified insulation foams, were tested alongside other phenolic and PIR foams and two non-combustible insulation boards, of glass wool (GW) and stone wool (SW).

The aim of this paper was to assess the fire safety of combinations of typical rainscreen façade products using micro-scale decomposition and bench-scale fire behaviour and toxic product evolution. The results are related to the large-scale government tests [12], following the Grenfell fire, on 8 m rainscreen façade systems.

2. Experimental

Commercial products designed for use in façade systems and the subject of this study are shown in Tables 1 and 2. They were analysed to determine their composition, thermal decomposition and fire behaviour. ACM_PE1, PF2 and PIR2 are reported to have been used extensively on the Grenfell Tower refurbishment. Other products have been selected to illustrate the range of different fire performance from different materials. The PIR2 product is unusual in that it has thin layers of glass wool sandwiched between thick (˜25 mm) layers of PIR foam.

For the ACM products, the aluminium sheets were removed in order to investigate the composition and micro-scale thermal decomposition of the filling material.

Table 1
Panel Materials.

Code	Filling	Density (kg m^{-3})	Thickness (mm)
ACM_PE1	PE	1400 (950*)	4
ACM_PE2	PE	1375 (925*)	4
ACM_FR1	PE with FR	1900 (1625*)	4
ACM_FR2	PE with FR	1900 (1650*)	4
ACM_FR3	PE with FR	1900 (1600*)	4
ACM_NC1	Mineral filled	1900 (1625*)	4
ACM_NC2	Corrugated aluminium	1100	4
HPL_PF	High pressure laminate (phenol formaldehyde)	1350	10
HPL_FR	High pressure laminate (phenol formaldehyde FR)	1350	8
MWB_1	Mineral wool board	1200	8
MWB_2	Mineral wool board	1250	9

* Measured density of filler material excluding aluminium.

Table 2
Insulation Materials.

Code	Description	Density (kg m^{-3})
PF1	Phenolic foam	42.8
PF2	Phenolic foam	41.8
PF3	Phenolic foam	45.0
PIR1	PIR foam	32.4
PIR2	PIR foam	35.0
PIR3	PIR foam	35.0
SW	Stone wool	37.0 (78.0)*
GW	Glass Wool	36.0

* Value reported is of lower density (insulating) layer, value in brackets is density of higher density external facing layer.

2.1. Elemental analysis

Outer-screen products, fillings for ACM products, and insulation boards were subject to elemental analysis using CHNS (Thermo Scientific Flash 2000 Organic Elemental Analyser), SEM-EDAX (FEI Quanta 200), and X-Ray fluorescence (Bruker Trace IV-SD handheld XRF) at 25 keV.

2.2. Polymer characterisation

The polymeric filling of the ACM_PE, ACM_FR and ACM_NC samples were characterised by diamond-attenuated total reflectance-FTIR spectrophotometry using a Nicolet IS 5 FTIR.

2.3. Thermal analysis

Samples of around 10 mg were subjected to thermogravimetric analysis (TGA) in air and nitrogen in a Stanton Redcroft STA 780, and differential scanning calorimetry (DSC) in a TA Instruments 2920, all at a heating rate of 10 °C min^{-1}.

2.4. Bomb calorimetry

The gross heat of combustion was measured in an oxygen bomb calorimeter (Parr 6200) according to ISO 1716:2002, running 2 replicate tests for each sample.

2.5. Microscale combustion calorimetry

Samples of around 2–3 mg were decomposed under pyrolysis and oxidative conditions (Method A and B in ASTM D7309 respectively) [13].

2.6. Cone calorimetry

All samples were tested at an applied heat flux of 50 kW m^{-2}, following ISO 5660 [14]. In order to investigate the burning behaviour of panel materials covered on both sides with 0.5 mm aluminium sheet, a novel methodology was devised, allowing the combustible contents to be ignited, while still testing a section of the whole panel. Outer-screen products of 70 × 70 mm^2, were placed centrally with the painted side uppermost in the 100 × 100 mm^2 sample holder. However, the results have been re-scaled so they are presented in kW m^{-2}. ACM products were tested complete with the aluminium sheets. The insulation materials were tested as blocks of 20 × 100 × 100 mm^3 cut from the larger boards, without the external aluminium foil facing. All samples were tested without the upper retaining frame. Where foam samples showed significant distortion, they were held in place using a wire grill specified in ISO 5660.

2.7. Smoke toxicity

The smoke toxicity of the insulation materials was determined using the steady state tube furnace (SSTF), following ISO TS 19700 [6] under the three flaming fire conditions described in ISO 19706 [7]: well-ventilated (stage 2); small under-ventilated (3a); and large under-ventilated (3b).

3. Results

3.1. Microscale decomposition

In the immediate aftermath of the Grenfell Tower fire, the UK government were advised to commission a series of initial screening tests on the combustibility of ACM filling samples taken from high-rise buildings [15] using bomb calorimetry. A summary of the findings from this screening is presented in the discussion. The heats of combustion of all products were measured using bomb calorimetry and microscale combustion calorimetry (MCC). The thermal decomposition in air and nitrogen was investigated for all ACM filling materials, outer-screen and insulation products. The data and commentary appears in SM.

3.1.1. Bomb calorimetry and microscale combustion calorimetry (Method B)

Table 3 shows the heat of combustion of each façade product or its filling (for ACM) determined by bomb calorimetry and MCC method B. The results show good agreement with the UK government data [12] and reasonable agreement between the bomb calorimeter and MCC method B, for the panel materials, discussed further in SM. The results show the very large contribution to heat release during combustion (measured by either method) from PE filled ACM and the significant reduction of adding 60% or more filler. The results also show the significant heat release of the plastic foam insulation per unit mass. The data are used to estimate the relative contributions to façade fires.

3.1.2. Microscale combustion calorimetry (Method a)

The rate of heat release following anaerobic pyrolysis of the panel fillings is shown in Fig. 2, with a peak of heat release under pyrolysis conditions for all ACM filler materials just below 500 °C. Method A is considered to be more representative of fire behaviour [16], as there is no oxygen between the flame and the fuel. The large and sharp peak of the PE filling is very significant, both to this work, and the Grenfell Tower fire. The total heat release is the area under each curve, and the peak is the pyrolysis temperature. For ACM, it shows the contribution different filler loadings make to the heat release rate, and that the peak decomposition temperature of the polymeric fuel is always close to 500 °C, except for the HPL products (HPL_PF, 350 °C and HPL_FR, 290 °C).

Table 3
Heat release of façade materials by bomb calorimetry and microscale combustion calorimetry (Method B).

Sample	Heat of Combustion: Bomb calorimetry /kJ g^{-1}	Heat of Combustion: Microscale combustion calorimetry /kJ g^{-1}
ACM_PE1	46.2	43.6
ACM_PE2	46.5	43.0
ACM_FR1	13.8	12.4
ACM_FR2	14.2	11.8
ACM_FR3	13.9	12.8
ACM_NC1	3.4	2.2
ACM_NC2	*	5.2
HPL_PF	21.3	19.3
HPL_FR	19.8	18.2
MWB_1	4.2	3.8
MWB_2	2.8	3.3
PF1	27.2	18.2
PF2	26.3	17.7
PF3	27.2	16.4
PIR1	28.1	21.9
PIR2	31.4	18.3
PIR3	29.8	23.7
SW	**	1.56
GW	2.43	1.95

* Corrugated aluminium could not be tested by bomb calorimetry as the metal oxidised too vigorously.

** A positive value of the heat of combustion could not be obtained from the stone wool sample, suggesting a very low binder content.

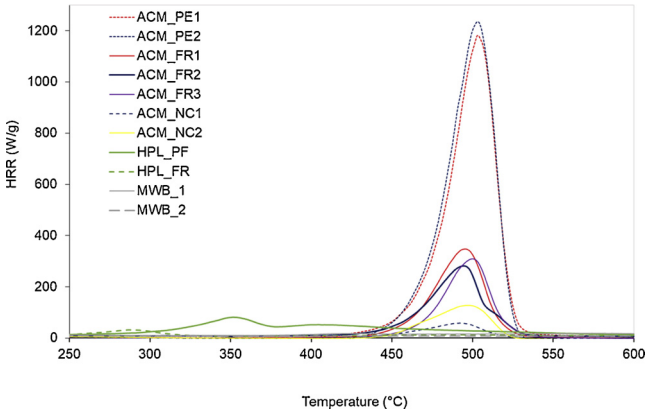

Fig. 2. Heat release of panel filling material by MCC Method A.

Fig. 3 shows very different rate of heat release data for the insulation, with much more gradual heat release occurring over the full temperature range (70 to 700 °C), compared to the outer-screen materials, and distinct peaks at 300 to 400 °C for PIR foams and at 500 °C for phenolic foams. The steady low heat release from the binders of the stone and glass wool show clear differences between these products and the foams.

3.2. Bench-Scale burning behaviour

3.2.1. Panel products

The novel methodology for testing sections of panel proved effective in assessing their contribution to the façade's flammability. The heat release rate (HRR) in cone calorimetry (Fig. 4) shows notable differences in combustibility of the different panels. All of the panel materials ignited in the cone calorimeter, although this only appeared to involve

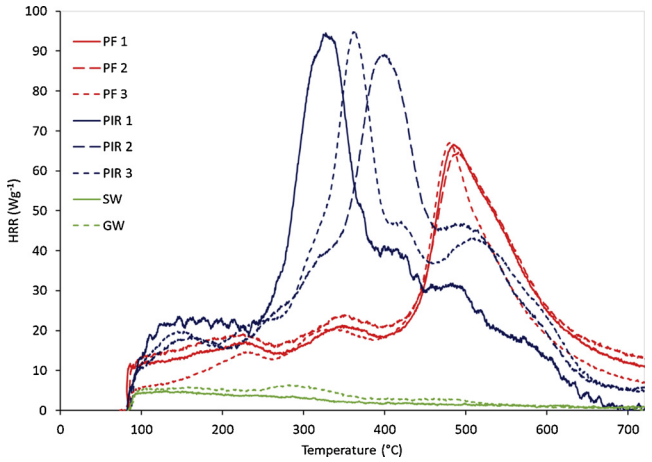

Fig. 3. Heat release of insulation materials by MCC Method A (note the use of different scales to Fig. 2).

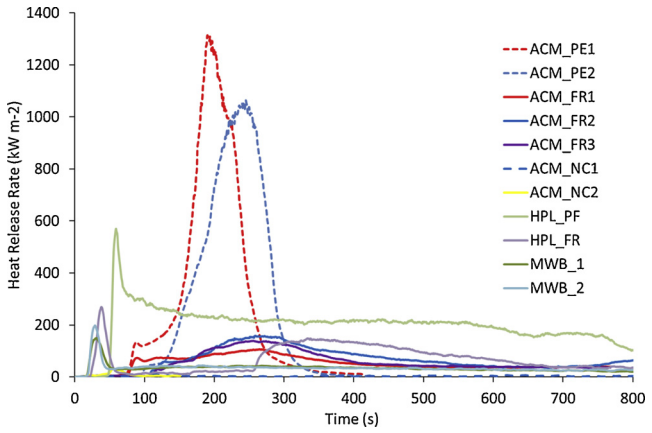

Fig. 4. HRR of 70 × 70 mm^2 panels in the cone calorimeter at 50 kW m^{-2}.

the paint finish for ACM_NC1 and NC2 and MWB_1 and MWB_2. High, sharp peaks of heat release rate were observed for ACM_PE1 and ACM_PE2, reaching a maximum of 1300 and 1050 kW m^{-2} at 190 and 250 s respectively. Moreover, ACM_PE1 and ACM_FR1, both from the same manufacturer, showed a notably earlier time to ignition than their competitor panels. Given this similarity of the TGA curves for these fillings, this suggests a thicker or more easily ignited paint layer, or a difference in absorptivity of radiant heat after the paint layers were burnt off. Almost no residue remained between the aluminium plates after the test for PE1 and PE2. The ACM_FRs underwent sustained flaming, but with a significantly lower HRR. It is clear that the combination of the protective aluminium sheets, and the metal hydroxide fire retardant at around 65% loading effectively reduces the flammability under these conditions. The $Al(OH)_3$ of ACM_FR2 is notably less effective than the $Mg(OH)_2$ of ACM_FR1 and ACM_FR3 at similar loadings.

3.2.2. Insulation

All the insulation foams show very rapid ignition and early peak HRR. However, the highest peaks are an order of magnitude less than those of the ACM_PE. Fig. 5 shows clear differences between the burning behaviour of PIR and phenolic foams. The PIRs show a higher initial peak HRR and lower steady burning rate, after formation of a protective char layer; the phenolic foams show a lower initial peak HRR but a higher steady burning rate. PIR2 was cut just below the glass wool layer; PIR2* was cut just above the glass wool layer to investigate its effect on the burning behaviour. This shows a slightly lower first peak HRR, but surprisingly, an enhanced second peak, at around 60 s A

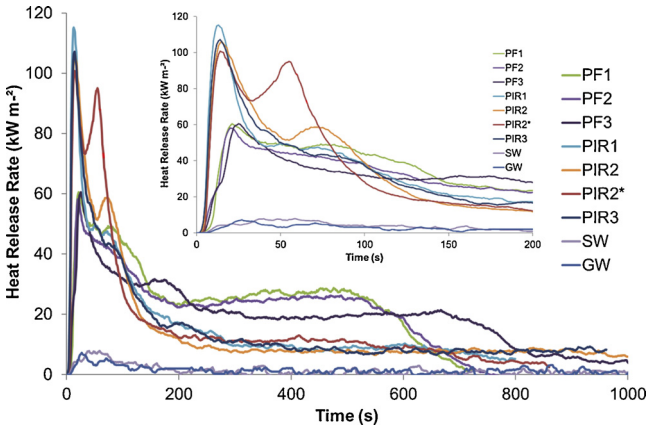

Fig. 5. HRR of insulation materials in the cone calorimeter at 50 kW m^{-2}. Inset shows early detail.

summary table of the parameters measured by cone calorimetry and a commentary on the data is provided in SM. A cone calorimetric study [17] of three commercial PIR and one phenolic foam showed similar results to those above, but highlighted the importance of the protective char layer on the burning behaviour.

3.3. The effect of ACM PIR combination

A qualitative experiment demonstrated the effect of combining ACM with PIR in a façade. A piece of ACM_PE (70 × 70 mm^2) was suspended 50 mm above a block of PIR (100 × 100 × 75 mm^3). Both products were mounted with their faces vertical. The ACM was heated with a small Bunsen flame until drips of the molten PE ignited. These fell onto the PIR and caused almost immediate ignition of the foam. The combination of the burning foam and the dripping PE rapidly led to self-sustaining combustion of the combination. This is illustrated in Fig. 6.

3.4. Bench-scale smoke toxicity

The SSTF yields are shown in Table 4. Each insulation product was burnt under three fire conditions, representing well-ventilated (ISO fire stage 2), small under-ventilated (3a) and large under-ventilated (3b). Only insulation products were investigated. The smoke toxicity of ACM fillings, and the yield data for insulation is discussed further in SM.

The HCN yields for phenolic foam are low, corresponding to their low nitrogen content, but increase with under-ventilation. The HCN yields for the PIR are significantly larger and increase by a factor of 2 to 4 in the transition from well-ventilated to under-ventilated.

The mineral wool insulation did not ignite, so its non-flaming combustion cannot be compared directly to the flaming combustion of the foams. However, they were tested under the three conditions used here for the combustible materials for completeness. The yields are all very low, as may be expected, and correspond to a small amount of binder, as seen in TGA and MCC etc. An attempt [18] to use the controlled atmosphere cone calorimeter [19] to assess the fire behaviour of PIR foam in under-ventilated conditions produced mixed results. As expected, the mass-loss fell with decreasing oxygen concentration, but surprisingly, the CO and HCN yields also fell, while the hydrocarbon yields increased, showing that flaming combustion was not the predominant gas phase process.

4. Discussion

Table 5 summarises the conclusions from the compositional analysis of the outer-screen products and fillings, based on manufacturer's information, analytical data and the reasoning presented in SM. The information is necessary in order to interpret their fire behaviour.

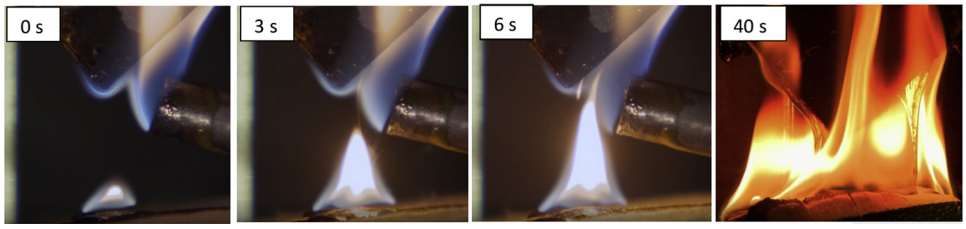

Fig. 6. Ignition of PIR by burning drips from ACM_PE showing time after first flaming drip.

The insulation materials are adequately described by the manufacturer's generic descriptions in Table 2.

The thermal decomposition data (from TGA) presented in SM, show good agreement with the micro-scale combustion data from MCC and bomb calorimetry. For the fillings, heat releases around 45, 13 and 3 kJ g^{-1} and mass losses of 95, 50 and 15% at 700 °C in nitrogen or air were found for the PE, FR and NC fillings respectively. The disproportionately higher mass losses for the FR materials correspond to the presence of aluminium and magnesium hydroxides which dehydrate on heating. For the insulation materials, the heat release in the bomb calorimeter is greater, mainly due to the more severe oxidation conditions than in the MCC. However, significantly less heat is released by the glass or stone wool samples than the combustible foams.

Table 5
Conclusions of screen product composition investigation.

Code	Filling/Composition
ACM_PE1	LDPE (100%)
ACM_PE2	LDPE (100%)
ACM_FR1	LDPE with 65-70% $Mg(OH)_2$
ACM_FR2	LDPE with 64-69% $Al(OH)_3$
ACM_FR3	LDPE with 65-71% $Mg(OH)_2$
ACM_NC1	LDPE (5%), $Al(OH)_3$ (15%), $Mg(OH)_2$ (33%), $CaCO_3$ (45%)
ACM_NC2	Aluminium (86%), epoxy resin (14%)
HPL_PF	Wood fibre bound with phenol-formaldehyde resin
HPL_FR	Fire retarded version of HPL_PF
MWB_1	Mineral fibre and organic binder (16%)
MWB_2	Mineral fibre and organic binder (9%)

4.1. Calculation of energy release

The heat release on complete combustion of the façade system has been estimated from its chemical composition and literature values, and from the measured values reported above. The façade system on the Grenfell Tower consisted of 3 mm PE sandwiched between two 0.5 mm sheets of aluminium on the outer face, with 160 mm of PIR insulation on the external face of the concrete. Using literature values for the density and heat of combustion of PE, PIR and aluminium respectively of 0.95 g cm^{-3} and 43 kJ g^{-1}; 0.0332 g cm^{-3} and 25 kJ g^{-1}; and 2.7 g cm^{-3} and 31 kJ g^{-1}, the heat release per unit area of façade on complete combustion of the PE is 123 MJ m^{-2}, for PIR it is 132 MJ m^{-2}, and for aluminium it is 84 MJ m^{-2}. Thus, on complete combustion, each square metre of the façade system can contribute 255 MJ (excluding aluminium) to 339 MJ (including aluminium) to the fire. Photographs of the burning Tower show falling sheets of aluminium and the debris at the foot of the Tower is littered with pieces of aluminium sheet [10], so it seems reasonable to conclude that the aluminium did not make a significant contribution to the heat release in situ.

In order to understand the burning behaviour of different combinations of building products, estimates of peak and total heat release have been made from small-scale tests. Table 6 shows the contribution to the heat release from each component of the façade system, as measured in the current work, using data on physical properties from Table 1 and 2, MCC,

Table 3, and cone calorimetry, Table S2, employing the approach described above. All insulation was calculated as 100 mm thick corresponding to the government tests [12].

Table 4
SSTF yield data 1.

Sample	ISO Fire Stage	Mass loss %	CO_2 Yield g/g	CO Yield g/g	HCN Yield g/g	HCl	NO	NO_2	H_3PO_4
PF1	2	97.5	2.509 ± 0.049	0.023 ± 0.007	< 0.001	0.001 ± 0.0001	< 0.001	< 0.001	< 0.001
	3a	72.7	0.495 ± 0.016	0.320 ± 0.003	0.001 ± < 0.0001	0.002 ± 0.0001	< 0.001	< 0.001	< 0.001
	3b	72.3	0.630 ± 0.029	0.280 ± 0.033	0.001 ± 0.0001	0.007 ± 0.0006	< 0.001	< 0.001	0.002 ± 0.0002
PF2	2	98.1	2.094 ± 0.351	0.031 ± 0.007	< 0.001	0.005 ± 0.0007	< 0.001	< 0.001	< 0.001
	3a	75.7	0.511 ± 0.019	0.282 ± 0.011	0.002 ± 0.0001	0.001 ± 0.0001	< 0.001	< 0.001	< 0.001
	3b	73.7	0.638 ± 0.058	0.229 ± 0.028	0.005 ± 0.0008	0.004 ± 0.0006	< 0.001	< 0.001	0.002 ± 0.0003
PF3	2	95.7	2.529 ± 0.099	0.028 ± 0.022	< 0.001	< 0.001	< 0.001	< 0.001	< 0.001
	3a	66.1	0.473 ± 0.072	0.317 ± 0.006	0.003 ± 0.0002	0.001 ± 0.0001	< 0.001	< 0.001	0.003 ± 0.0002
	3b	63.6	0.562 ± 0.187	0.223 ± 0.014	0.003 ± 0.0003	0.001 ± 0.0001	< 0.001	< 0.001	0.001 ± 0.0001
PIR1	2	95.3	2.077 ± 0.045	0.106 ± 0.028	0.006 ± 0.0003	0.008 ± 0.0004	< 0.001	< 0.001	< 0.001
	3a	76.6	0.610 ± 0.040	0.217 ± 0.070	0.011 ± 0.0009	0.005 ± 0.0004	0.001 ± 0.0001	< 0.001	< 0.001
	3b	78.9	0.554 ± 0.025	0.416 ± 0.048	0.015 ± 0.0008	0.003 ± 0.0002	0.002 ± 0.0001	< 0.001	0.001 ± 0.0001
PIR2	2	92.0	2.376 ± 0.080	0.014 ± 0.007	0.004 ± 0.0001	0.013 ± 0.0004	< 0.001	< 0.001	< 0.001
	3a	75.9	0.447 ± 0.013	0.340 ± 0.031	0.017 ± 0.0010	0.006 ± 0.0003	0.003 ± 0.0002	< 0.001	< 0.001
	3b	74.4	0.520 ± 0.061	0.341 ± 0.085	0.014 ± 0.0032	0.007 ± 0.0016	0.001 ± 0.0002	< 0.001	< 0.001
PIR3	2	94.4	2.375 ± 0.024	0.037 ± 0.014	0.004 ± 0.0002	0.019 ± 0.0011	< 0.001	< 0.001	0.002 ± 0.0001
	3a	77.4	0.511 ± 0.054	0.331 ± 0.049	0.014 ± 0.0006	0.006 ± 0.0003	0.002 ± 0.0001	< 0.001	0.001 ± 0.0001
	3b	78.9	0.652 ± 0.056	0.249 ± 0.025	0.014 ± 0.0004	0.004 ± 0.0001	< 0.001	< 0.001	< 0.001
SW*	2 – NF	1.77	0.027 ± 0.007	0.010 ± 0.002	< 0.001	< 0.001	< 0.001	< 0.001	< 0.001
	3a – NF	1.67	0.020 ± 0.006	0.009 ± 0.001	< 0.001	< 0.001	< 0.001	< 0.001	< 0.001
	3b – NF	1.64	0.051 ± 0.011	< 0.001	< 0.001	< 0.001	< 0.001	< 0.001	< 0.001
GW*	2 – NF	6.21	0.093 ± 0.018	0.018 ± 0.003	< 0.001	< 0.001	< 0.001	< 0.001	< 0.001
	3a – NF	8.63	0.144 ± 0.015	0.011 ± 0.001	< 0.001	< 0.001	< 0.001	< 0.001	< 0.001
	3b – NF	12.7	0.189 ± 0.024	< 0.001	< 0.001	< 0.001	< 0.001	< 0.001	< 0.001

* Also tested at 900 °C but did not ignite; NF = not flaming.

Table 6
Potential heat release from each component of the façade system.

Sample	Cone calorimeter data		MCC data
	Peak HRR /kW m^{-2}	Total heat release /MJ m^{-2}	Total heat release /MJ m^{-2}
ACM_PE1	1364	105.4	124
ACM_PE2	1123	106.6	119
ACM_FR1	123	59.6	60
ACM_FR2	195	70.9	58
ACM_FR3	144	65.07	61
ACM_NC1	13.8	2.57	11
ACM_NC2	30.2	0.87	17
HPL_PF	530	172.71	260
HPL_FR	263	67.49	196
MWB_1	150	37.03	36
MWB_2	194	27.75	38
PF1	63.7	18.71	78
PF2	62.0	17.56	74
PF3	64.8	19.67	74
PIR1	116	13.33	71
PIR2	106	15.6	64
PIR3	107	14.5	83
SW	5.6	0.06	9
GW	8.7	0.67	7

4.2. Correlation of micro- and bench-scale results to DCLG tests

In order to link the government test results [12] to the fire behaviour observed in this study, the potential contribution to flame spread has been estimated, based on the data measured here. Two methodological approaches were used. The first calculated the total energy release from the heat of combustion data, per m^2 of façade, from MCC method B data, and cone calorimetry. The second used the sum of the pHRR from the products, in kW m^{-2} from cone calorimetry, since the pHRR drives fire growth [20]. Table 7 shows the potential heat release by each component of the façade system used in the government BS8414-1 tests. A critique of the BS 8414 standard, the BR 135 criteria, and the DCLG tests has been reported elsewhere [21].

This very crude assessment is based on the large contribution to the peak of heat release from the PE flowing out of the ACM and the smaller contribution to peak heat release rate from the burning insulation material. The ACM_FR + PF of test 7 performed better than the ACM_FR and PIR of test 3 inasmuch as the thermocouples recorded a 600 °C rise for 30 s at 1530s, rather than 1220s, although the test criteria [22] only consider temperatures exceeding 600 °C for the first 15 min (900 s) of the test.

In the aftermath of the Grenfell Tower fire, the test results for three other cladding systems meeting the test criteria were made publicly available: two use stone wool, one with ACM_FR, the other with ACM_NC, for which our simple method predicts a pass. Another system used ACM_FR with PF insulation, similar to that which failed in the government tests due to “flame spread above the test apparatus”. This system has the lowest total peak HRR from cone calorimetry (212 kW m^{-2}) of those failing the government test. Thus, the use of total peak HRR from cone calorimetry or MCC appears to be as good a predictor of behaviour in rainscreen façade systems as the BS 8414-1 test. The cost of these tests is around 0.01 of the large-scale tests.

No BS 8414-1 test reports appear to have been made publically available for HPL screened systems, although they are widely used in rainscreen systems on multi-storey residential buildings. Using the data reported here, and the thresholds for passing the DCLG test, the performance in the large-scale test of HPL_PF, HPL_FR and MWB1 and 2 outer-screens and different insulation products is predicted in Table 8. The intermediate values in Table 7 for heat of combustion in MCC, 100 kW m^{-2}, cone calorimeter, 68 kW m^{-2}, and peak HRR, 157 kW m^{-2} have been used as pass/fail criteria.

It is apparent that none of the HPL_PF or HPL_FR screened systems would be expected to pass using any of the three criteria, while consistent predictions were not found from any of the MWB combinations, except MWB1 with SW. Since the peak HRRs for MWB screens result from burning paint, they are probably unrepresentative of the large-scale test performance.

Thus, the differences in fire behaviour between the combustible materials and non-combustible materials are so great that they can easily be quantified using tests costing hundreds of pounds or less, rather than the tens of thousands of pounds required to run a single BS 8414-1 test. In addition, the robustness of the bench-scale material tests prevents misleading test results from being reported, based on optimising the design of the façade system to pass the test, irrespective of how representative it is of actual building façades. It is important to note that the design and construction of the façade for the test is normally the responsibility of the product manufacturer, not the test laboratory. The Forum of Fire Testing Laboratories [23] proposed the use of microscale decomposition and numerical models to replace large-scale fire tests, and thus eliminate these sorts of problems, over a decade ago.

In a study sponsored by the insulation manufacturer, Kingspan, Guillaume [24] argues that only the fire performance of the whole façade need be considered, not the individual components. The tests used a 2.4 m ACM rainscreen façade (following ISO 13785-1), fitted with cavity barriers, using a fire source of 100 kW and a 2 mm aluminium protective L-profile, and only the ACM made a significant contribution to the burning behaviour. However, the test claims to be a ⅓rd-scale BS8414-1, while the fire source is only $^{1}/_{30}^{th}$ of BS8414-1, which does not test the façade system adequately.

4.3. Smoke toxicity

As discussed in SM, the fire condition and hence the toxicity of burning ACM fillings on the side of a building is too difficult to predict from bench-scale experiments. The burning of the PIR and phenolic foam behind the ACM on Grenfell Tower would almost certainly have been under-ventilated (uv) between fire stages 3a and 3b. Fig. 7 shows the relative contribution to incapacitation of HCN and CO from burning 1 kg of insulation material after 5 min exposure under the stated fire

Table 7
Predicted behaviour of combinations of façade components, and comparison with government test results [12], in order of fire performance.

Test number	Products in test	UK government test result (BS8414-1)	Σ(Heat of combustion per unit area) MCC method B / kW m^{-2}	Σ(Heat of combustion per unit area) cone calorimeter / kW m^{-2}	Σ(Peak Heat Release Rate) cone calorimeter / kW m^{-2}
1	ACM PE + PIR	Test stopped (9 min)	188	121	1471
2	ACM PE + SW	Test stopped (7 min)	134	105	1370
3	ACM FR + PIR	Test stopped (25 min)	125	75	230
7	ACM FR + PF	Test stopped (28 min)	134	77	185
4	ACM FR + SW	Test passed	70	60	129
5	ACM NC + PIR	Test passed	75	18	120
6	ACM NC + SW	Test passed	20	3	19

Table 8
Predicted behaviour of combinations of façade with HPL panels.

Products in test	Σ(Heat of combustion per unit area) MCC method B / kW m^{-2}	Pass/Fail (Pass < 100)	Σ(Heat of combustion per unit area) cone calorimeter / kW m^{-2}	Pass/Fail (Pass < 68)	Σ(Peak Heat Release Rate) cone calorimeter / kW m^{-2}	Pass/Fail (Pass < 157)
HPL_PF + PIR	324	✗	188	✗	636	✗
HPL_PF + SW	270	✗	173	✗	535	✗
HPL_PF + PF	334	✗	190	✗	592	✗
HPL_FR + PIR	261	✗	83	✗	370	✗
HPL_FR + SW	206	✗	68	✗	269	✗
HPL_FR + PF	270	✗	85	✗	325	✗
MWB1 + PIR	101	✗	53	✓	256	✗
MWB1 + SW	46	✓	37	✓	155	✓
MWB1 + PF	110	✗	55	✓	212	✗
MWB2 + PIR	102	✗	43	✓	300	✗
MWB2 + SW	47	✓	28	✓	199	✗
MWB2 + PF	112	✗	45	✓	256	✗

condition with the effluent dispersed over a volume of 50 m^3 (a large room or small apartment) based on ISO 13571. Burning this amount of phenolic foam in uv conditions is predicted to cause incapacitation to somewhat less than 50% of the exposed population, as the FED is less than one. However, burning this amount of any of the three PIR foams used in this study would exceed the threshold for incapacitation by a factor of between 2 and 4 in uv conditions. The higher toxicity of PIR results from the presence of nitrogen in the polymer, which forms HCN on burning, particularly in uv conditions. Once incapacitation has occurred (in this case HCN causes loss of consciousness), the victim can no longer effect of their own escape, and unless rescued, will continue to uptake CO and HCN until breathing ceases.

Fig. 8 shows the prediction of lethality from the same effluents. This shows a similar trend to that of incapacitation in Fig. 7, but the relative contribution of HCN to CO is reduced. However, HCN still makes a significant contribution to the toxicity of the effluents from all the foams, far exceeding the toxicity from CO for under-ventilated burning of the PIR foams. The FED for lethality is calculated from ISO 13,344, based on a 30 min exposure time. The low levels of binder in SW and GW generate correspondingly low levels of asphyxiants, and low toxicity. Coupled with their inability to propagate combustion, this shows why they are a safe alternative to combustible insulation. The material-IC_{50} and material-LC_{50} values discussed in SM and shown in Table S4 provide the most direct route to estimating a safe loading of insulation material.

4.4. The extent of the ACM problem

The government has established that there are 478 residential buildings over 18 m with ACM cladding [15] in England. 150 are in private ownership and are believed to be non-compliant, but fuller data is unavailable. Fig. 9 shows that for the remaining 328, 85% have ACM_PE combined with combustible foam (29%), mineral wool (34%) and unknown (23%). A minority (14%) have ACM_FR with different types of insulation, but none have ACM with a non-combustible core (ACM_NC).

Of the 328 buildings for which data is available, 316 do not comply with the UK Building Regulations. Of the non-compliant buildings, half are social housing (50%) with the remainder divided between student residences, and other public and private buildings, Fig. 10.

A consultation document on the future of desktop studies (described in SM) showed that the government expected around 600 tall buildings per year to have combustible facades [25]. This includes buildings with rainscreen (or ventilated) façades clad with HPL etc., and External Thermal Insulation Composite Systems (ETICS) type façades, where a lightweight cement render covers the combustible insulation. Since combustible building exteriors have been permitted since 2006, if they became established building practice 10 years ago, this estimate suggests there could be as many as 6000 buildings over 18 m in England with combustible façades.

5. Conclusions

In the aftermath of the Grenfell Tower tragedy there are a number of unanswered questions. This study came about because of the lack of published information relating to the composition, decomposition and fire behaviour of available façade products, and the dependence on controversial large-scale tests. This paper provides that crucial information, and demonstrates its relationship to large-scale test performance. Moreover, the data show good consistency between scales and different decomposition conditions. It highlights large differences in fire behaviour between different products, both for outer-screens and

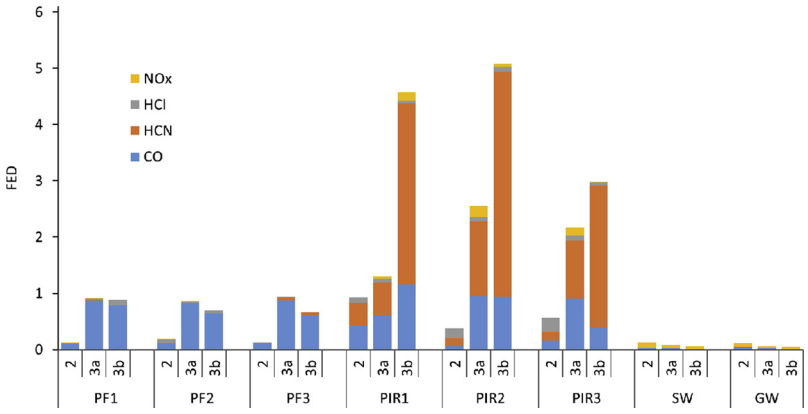

Fig. 7. FED for incapacitation following 5 min exposure from burning 1 kg with the effluent dispersed in a volume of 50 m^3.

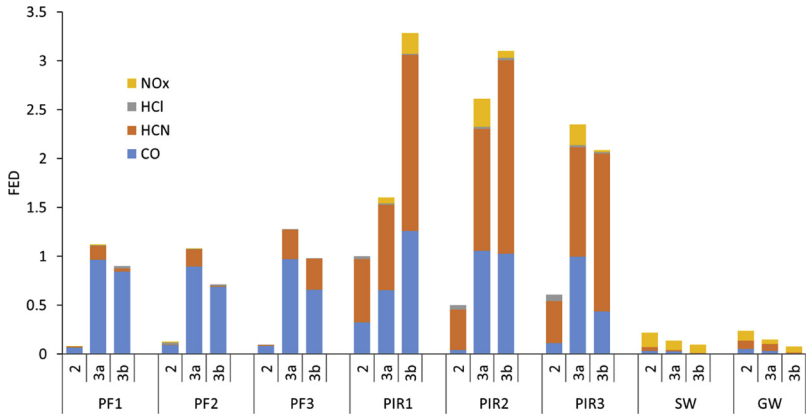

Fig. 8. 30 min lethal FED (ISO 13344) from burning 1 kg with the effluent dispersed in a volume of 50 m^3.

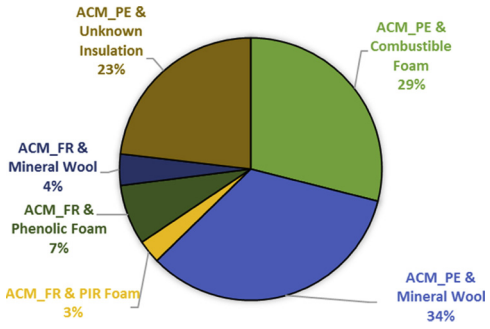

Fig. 9. Tall buildings in England with ACM panels.

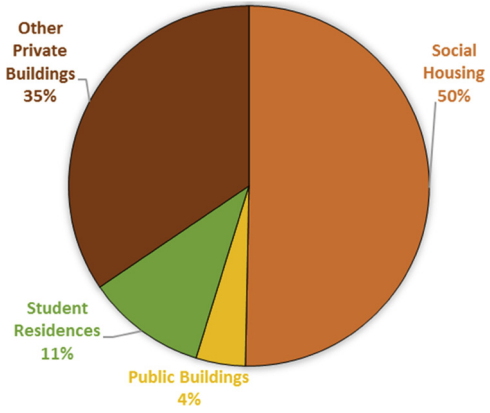

Fig. 10. Use of tall buildings not meeting Building Regulations.

insulation boards.

By comparing similar products of the same generic type (e.g. ACM_FR, or PIR) it shows that there is little difference in the decomposition and burning behaviour for that product type, and also in the case of the insulation materials, in the smoke toxicity.

The bench-scale burning behaviour shows the most dramatic differences between the ACM_PE and the ACM_FR and ACM_NC materials. This illustrates clearly how ACM_PE contributes to very rapid fire spread when used to clad the exterior of a building. It also identifies a potential problem with HPL_PF. The bench-scale burning behaviour of the PIR and PF shows the contrasting effect of the more resilient char on the PIR (higher initial peak followed by lower HRR) compared to the PF (lower peak HRR but a higher steady HRR). This difference is demonstrated by the TGA in air, where the mass loss rate of the PIR is initially higher, but around 450 °C the PF overtakes it. The lack of heat release from the stone and glass wool materials is expected, but is crucially important in understanding how to prevent further tragedies, demonstrating the existence of alternative non-combustible insulation materials.

In the under-ventilated conditions of flaming within the cavity, the smoke toxicity data show a factor of 3 increase for PIR, compared to PF. The non-combustible GW and SW products show smoke toxicity lower than the PIR by a factor of around 15. Again, these results have very clear implications for those selecting products to ensure the fire safety of occupants.

The simple additive models of total heat release and peak HRR underline the effects of large differences in fire behaviour, and allow elimination of the most dangerous combinations from façades. In contrast, the qualitative demonstration of PIR ignition by flaming drips of PE from ACM serves as a warning to treat systems as a whole, rather than the sum of their individual parts, since one component can interact synergistically or antagonistically with any other. The evidence presented in this paper challenges the statements such as “the test results with regard to heat release rates, smoke and toxic gas emissions show that the organic polyisocyanurate insulation and the mineral fibre insulation behave similarly during the fire” made by the combustible foam industry [26], that their insulation products do not constitute a safety hazard

If the data in this paper had been readily available, it may have contributed to the prohibition of combustible materials on the outside of tall buildings, as they are in most of Europe, and this tragedy could not have occurred. In the UK, the building fire regulations have just been modified to ban the use of combustible materials on the outside of tall buildings (November 2018) [27].

Acknowledgements

SO would like to thank the University of Bologna for funding a student exchange. No other external funding from any source was used to support this project.

Appendix A. Supplementary data

Supplementary material related to this article can be found, in the online version, at doi:https://doi.org/10.1016/j.jhazmat.2018.12.077.

References

[1] UK Fire Statistics 2017 and Preceding Editions, Home Office, London, https://www.gov.uk/government/collections/fire-statistics (Accessed 8/12/2018).
[2] J.R. Hall, Fatal Effects of Fire, National Fire Protection Association, Quincy, MA, 2011.
[3] ISO 13571, Life-threatening Components of Fire - Guidelines for the Estimation of Time to Compromised Tenability in Fires, ISO, Geneva, 2012.
[4] ISO 13344, Estimation of the Lethal Toxic Potency of Fire Effluents, ISO, Geneva, 2015.
[5] T.R. Hull, A.A. Stec, K. Lebek, D. Price, Factors affecting the combustion toxicity of

polymeric materials, Polym. Degrad. Stab. 92 (12) (2007) 2239–2246, https://doi.org/10.1016/j.polymdegradstab.2007.03.032.
[6] ISO/TS 19700, Controlled Equivalence Ratio Method for the Determination of Hazardous Components of Fire Effluents - Steady-state Tube Furnace, ISO, Geneva, 2016.
[7] ISO 19706, Guidelines for Assessing the Fire Threat to People, ISO, Geneva, 2011.
[8] W.D. Woolley, M.M. Raftery, Smoke and toxicity hazards of plastics in fires, J. Hazard. Mater. 1 (3) (1975) 215–222, https://doi.org/10.1016/0304-3894(75)80014-8.
[9] Anna A. Stec, T. Richard Hull, Assessment of the fire toxicity of building insulation materials, Energy Build. 43 (2011) 498–506, https://doi.org/10.1016/j.enbuild.2010.10.015.
[10] Dr Barbara Lane, Expert Witness Report, https://www.grenfelltowerinquiry.org.uk/evidence/dr-barbara-lanes-expert-report (Accessed 25/06/2018).
[11] T.R. Hull, A. Witkowski, L. Hollingbery, Fire retardant action of mineral fillers, Polym. Degrad. Stab. 96 (8) (2011) 1462–1469, https://doi.org/10.1016/j.polymdegradstab.2011.05.006.
[12] DCLG Fire Test Reports, (2017) (accessed 8/12/2018), https://www.gov.uk/government/news/latest-large-scale-government-fire-safety-test-result-published.
[13] ASTM D7309-13, Standard Test Method for Determining Flammability Characteristics of Plastics and Other Solid Materials Using Microscale Combustion Calorimetry, ASTM International, West Conshohocken, PA, 2013.
[14] ISO 5660-1, Reaction-to-fire Tests — Heat Release, Smoke Production and Mass Loss Rate — Part 1: Heat Release Rate (cone Calorimeter Method) and Smoke Production Rate (dynamic Measurement), ISO, Geneva, 2015.
[15] MHCLG Building Safety Programme: Monthly Data Release – August 2018, and preceding editions. https://www.gov.uk/government/publications/building-safety-programme-monthly-data-release-august-2018 (Accessed 8/12/2018).
[16] B. Schartel, T.R. Hull, Development of fire-retarded materials - Interpretation of cone calorimeter data, Fire and Mater. 31 (5) (2007) 327–354, https://doi.org/10.1002/fam.949.
[17] J.P. Hidalgo, J.L. Torero, S. Welch, Fire performance of charring closed-cell polymeric insulation materials: polyisocyanurate and phenolic foam, Fire and Mater. 42 (4) (2018) 358–373, https://doi.org/10.1002/fam.2501.
[18] D.M. Marquis, F. Hermouet, É. Guillaume, Effects of reduced oxygen environment on the reaction to fire of a poly(urethane-isocyanurate) foam, Fire and Mater. 41 (3) (2017) 245–274, https://doi.org/10.1002/fam.2378.
[19] V. Babrauskas, W.H. Twilley, M. Janssens, S. Yusa, A cone calorimeter for controlled-atmosphere studies, Fire and Mater. 16 (1) (1992) 37–43, https://doi.org/10.1002/fam.810160106.
[20] V. Babrauskas, R.D. Peacock, Heat release rate: the single most important variable in fire hazard, Fire Saf. J. 18 (3) (1992) 255–272, https://doi.org/10.1016/0379-7112(92)90019-9.
[21] J. Schulz, D. Kent, A. Crimi, T.R. Hull, A Critical Review of the UK's Regulatory Regime for Combustible Façades, Submitted to Fire Technology, August (2018).
[22] S. Colwell, T. Baker, BR 135: Fire Performance of External Thermal Insulation for Walls of Multistorey Buildings, BRE Trust, Watford, (2013).
[23] R.G. Bill Jr, P.A. Croce, The International FORUM of Fire Research Directors: a position paper on small-scale measurements for next generation standards, Fire Saf. J. 41 (7) (2006) 536–538, https://doi.org/10.1016/j.firesaf.2006.05.005.
[24] E. Guillaume, T. Fateh, R. Schillinger, R. Chiva, S. Ukleja, Study of fire behaviour of facade mock-ups equipped with aluminium composite material-based claddings, using intermediate-scale test method, Fire and Mater. 42 (5) (2018) 561–577, https://doi.org/10.1002/fam.2635.
[25] MHCLG Amendments to statutory guidance on assessments in lieu of test in Approved Document B (Fire Safety): A consultation paper https://www.gov.uk/government/consultations/approved-document-b-fire-safety-amendments-to-statutory-guidance-on-assessments-in-lieu-of-tests (Accessed 8/12/2018).
[26] R. Weghorst, E. Antonatus, S. Kahrmann, C. Lukas, J. Bulk, An investigation into the relevance of the contribution to toxicity of different construction products in a furnished room fire, 15th International Conference and Exhibition on Fire and Materials 2017 1 (2017) 352–363.
[27] Ministry of Housing, Communities & Local Government, UK, Guidance: Ban on Combustible Materials, (2018) November (Accessed 8/12/2018) https://www.gov.uk/guidance/ban-on-combustible-materials.